Chapter 4

The deterministic limit $p \to 0$

As a first step to understand the model introduced in the last chapter, one can start with its deterministic limit, i.e. $p \to 0$, which simply amounts to taking the randomization rule out of the velocity update. It will turn out that this limit already contains many of the properties of the complete CA model, albeit in a deterministic way. This is not realistic, but easy to work with. Most traffic models used in the Statistical Physics literature so far do not go beyond this model [15, 17, 116, 172, 182], although it is often used in two dimensions [17, 30, 112, 118, 119, 166].

Further results with the deterministic model, for example on different update schemes, and more details of the following can be found in [121].

4.1 Fundamental diagram and phenomenological behavior

The fundamental diagram for the deterministic limit simply consists of two straight lines (Fig. 4.1), which intersect at $\rho_{c,det} = \rho(q_{max}) = 1/6$ and $q_{c,det} = q_{max,det} = 5/6$. They will be explained further down. The intersection point divides two phenomenological regimes: light traffic ($\rho < \rho_{c,det}$) and dense traffic ($\rho > \rho_{c,det}$). A typical situation for light traffic is shown in Fig. 4.2. After starting from a random initial condition, the traffic relaxes to a steady state, where the whole pattern just moves $v_{max} = 5$ positions to the right in each iteration. Cars clearly have a tendency of keeping a *gap* of $\geq v_{max} = 5$ between each other. As a result, the current q in this regime is

$$q_< = \rho \cdot v_{max} \ .$$

The velocity of the kinematic waves in this regime is $c_< = q'_< = v_{max}$. This means that disturbances, such as holes, just move with the traffic, as can also be seen in Fig. 4.2.

Dense traffic is different (Fig. 4.3). Again starting from a random initial configuration, the simulation relaxes to a steady state where the whole pattern moves one position to the *left* in each iteration. Note that cars still move to the right; if one follows the trajectory of one individual vehicle, for this car regions of relatively free movement are alternating with regions of high density and slow speed. Although in a too static way, this captures some of the features of start-stop-traffic. The average speed in the steady state equals the number of empty sites divided by the number of particles: $\langle v \rangle_L = (L-N)/N$; the current is $q_> = \rho \cdot \langle v \rangle_L$, or, with $\rho = N/L$,

$$q_> = 1 - \rho \ .$$

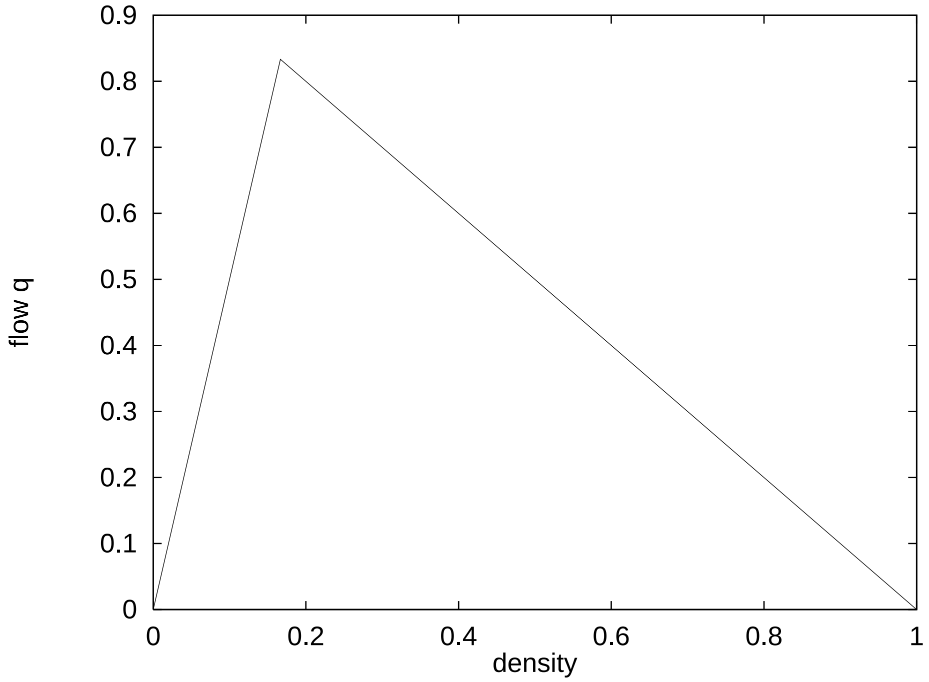

Figure 4.1: Flow-density relation for the deterministic limit.

```
...........5.....1.1.1.............4....5............4.....3..........
................1.1.1.2................5.....5...........4....4.......
.................1.1.2..3...................5.....5..........4....5...
.5................1.2..3...4.....................5.....5.........5....
5.....5............2..3...4....5......................5.....5.........
.....5.....5.........3...4....5.....5......................5.....5....
5.........5.....5.......4....5.....5.....5......................5.....
                              now steady
.....5.........5.....5......5.....5.....5.....5......................5
....5.....5.........5.....5......5.....5.....5.....5..................
.........5.....5.........5.....5......5.....5.....5.....5.............
..............5.....5.........5.....5......5.....5.....5.....5........
...................5.....5.........5.....5......5.....5.....5.....5...
.5......................5.....5.........5.....5......5.....5.....5....
5.....5......................5.....5.........5.....5......5.....5.....
.....5.....5......................5.....5.........5.....5......5.....5
....5.....5.....5......................5.....5.........5.....5......5.
...5.....5.....5.....5......................5.....5.........5.....5...
```

Figure 4.2: Evolution of the deterministic model from random initial conditions for low density ($\rho < \rho(q_{max})$). Note the quick relaxation towards a steady state.

This straight line intersects with the one from light traffic at $\rho_{c,det} = 1/(1 + v_{max})$, which is therefore the density corresponding to maximum throughput.

The velocity of the kinematic waves in the dense regime is $q'_{>} = -1$, which corresponds to the backwards moving pattern in Fig. 4.3.

```
..........1.1.4....03...2..4....04.......4....1.1.4....00..5.....01.1.
...........1.2....01...2..3....01....5.......1.1.2....001.......01.1.2
.3..........2..2..1.2....3...1.1.2........3...1.2..2..01.2......1.1.2.
3...4.........2..1.2..3.....1.1.2..3.........1.2..2..01.2..3.....1.2..
...4....5.......1.2..3...3...1.2..3...4.......2..2..01.2..3...3...2..3
..4....5.....3...2..3...3...1.2..3...4....5.....2..01.2..3...3...2..3.
                          now steady
.4....5.....3...2..3...3...1.2..3...4....5.....2..01.2..3...3...2..3..
4....5.....3...2..3...3...1.2..3...4....5.....2..01.2..3...3...2..3...
....5.....3...2..3...3...1.2..3...4....5.....2..01.2..3...3...2..3...4
...5.....3...2..3...3...1.2..3...4....5.....2..01.2..3...3...2..3...4.
..5.....3...2..3...3...1.2..3...4....5.....2..01.2..3...3...2..3...4..
 disturbing here:        x
.5.....3...2..3...3...1.1..3...4....5.....2..01.2..3...3...2..3...4...
5.....3...2..3...3...1.1.2....4....5.....2..01.2..3...3...2..3...4....
.....3...2..3...3...1.1.2..3......5.....2..01.2..3...3...2..3...4....5
....3...2..3...3...1.1.2..3...4........2..01.2..3...3...2..3...4....5.
...3...2..3...3...1.1.2..3...4....5......01.2..3...3...2..3...4....5..
..3...2..3...3...1.1.2..3...4....5.....1.1.2..3...3...2..3...4....5...
                   now steady again, damage time:  5
.3...2..3...3...1.1.2..3...4....5.....1.1.2..3...3...2..3...4....5....
3...2..3...3...1.1.2..3...4....5.....1.1.2..3...3...2..3...4....5.....
```

Figure 4.3: Evolution of the deterministic model from random initial conditions for high density ($\rho > \rho(q_{max})$). Note the quick relaxation towards a steady state, which, though, looks different than for light traffic (Fig. 4.2). The disturbance changes the wave where it happens, and causes a hole moving downstream which is absorbed by the next wave.

4.2 Damage times

In order to estimate the duration of a disturbance, a "damage time" τ_d [159] was measured in the simulation model. To do so, after reaching the steady state, the velocity of one randomly chosen particle is reduced by the smallest possible amount (i.e. by one); the damage time τ_d then is the time the system needs to reach again a new steady state. As explained, the steady state is reached when the entire configuration of the system at time $t+1$ either is a right (v_{max} positions) or a left (1 position) shift of the configuration at time t.

Numerical results for τ_d as a function of the density $\rho = N/L$ are given in Fig. 4.4. At the density $\rho_{c,det} = 1/6$ the damage time τ_d shows a remarkable peak which grows with system size; finite size scaling analysis confirms that it diverges as

$$\tau_d(\rho_c) \propto L \ .$$

The phenomenological reason for the divergence at $\rho_c = 1/6$ for the parallel update is as follows. At first, note that each disturbance can produce both a "hole", which moves with v_{max}, and a "front", which moves backwards as a kinematic wave.

- At low densities, the front travels upstream and is absorbed by a gap; the relevant length scale obviously depends on ρ and not on L. The "hole" will survive forever, thus having no influence on stationarity.
- For high densities (compare Fig. 4.3), the situation is inverse: The new front survives forever, whereas the hole is absorbed by the next wave. The length scale for the wave similarly depends on ρ.
- In between the high and the low density regimes, a transition takes place; and the critical point is a state where particles move with maximum velocity $v_{max} = 5$ and minimum gap

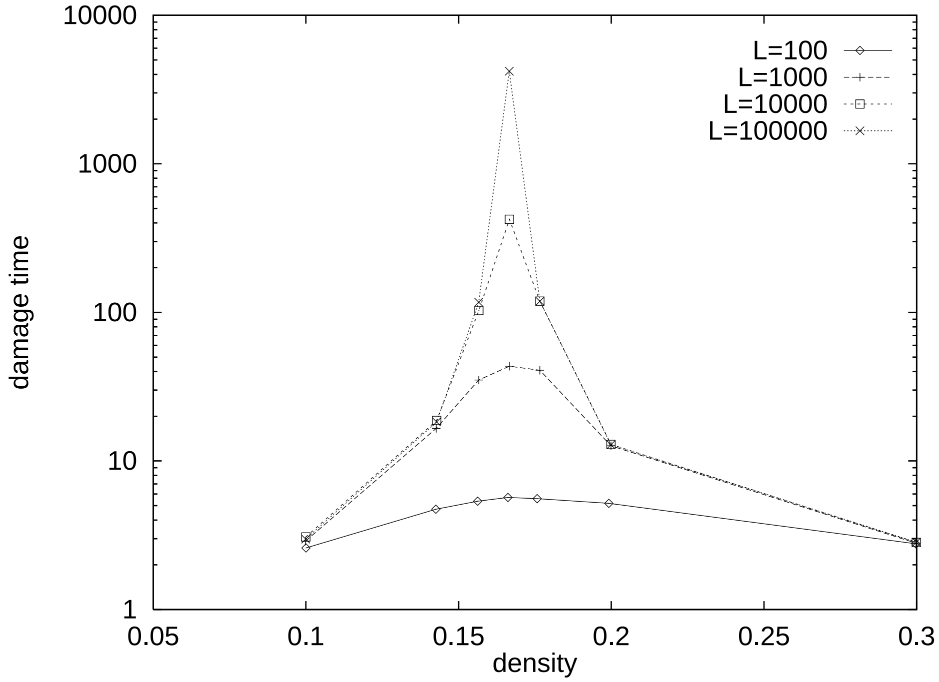

Figure 4.4: Relaxation times after disturbing for traffic in a closed system using the deterministic model, for different densities and different system sizes L. Note that the system size is only relevant for densites near $\rho(q_{max}) = 1/6$.

$gap_{min} = v_{max} = 5$ (and therefore $\rho_c = 1/(gap_{min} + 1) = 1/6$). If one introduces a disturbance into this "critical" state, front and hole move in opposite direction until they meet again (periodic boundary conditions!); hence the L-dependance of τ_d at ρ_c.

At the same time, ρ_c is the density which corresponds to maximum particle throughput.

4.3 Self-organization of the critical state

If one assumes a very dense jam as in Fig. 4.5, then the outflow from this jam assumes exactly the critical configuration of particles moving at maximum speed 5 and with $gap = 5$. This is no longer true for an open boundary which is fixed in space (Fig. 4.6); but it can be restored, e.g., by forcing a higher acceleration for the first particle (Fig. 4.7). In this last case, a disturbance (as in Fig. 4.7) causes a front which travels with constant speed to the left boundary, whereas the hole travels with constant speed to the right boundary. Conceptually, this case of self-organized criticality therefore belongs to Bak, Tank, and Wiesenfeld's one-dimensional sandpile model [8], with the difference that our model selects a state of non-trivial density (i.e. $\rho_c \neq 0$).

With respect to reality, this means that the outflow of the traffic jam adjusts itself exactly at the critical density and therefore at maximum capacity, and due to the criticality, new disturbances have long-ranged effects through density waves traveling with constant speed. This is no longer true for a bottleneck situation (e.g. a two-lane directional road merging into only one lane): The open boundary described in Fig. 4.6 leads to lower density and throughput, and the same is true similarly for the full CA model (see later) and for reality.

```
00000000000000000000000001.2..3...4....5.....5.....5.....5.....5.....5
0000000000000000000000001.2..3...4....5.....5.....5.....5.....5.....5.
000000000000000000000001.2..3...4....5.....5.....5.....5.....5.....5..
00000000000000000000001.2..3...4....5.....5.....5.....5.....5.....5...
0000000000000000000001.2..3...4....5.....5.....5.....5.....5.....5....
000000000000000000001.2..3...4....5.....5.....5.....5.....5.....5.....
0000000000000000001.2..3...4....5.....5.....5.....5.....5.....5.....5
000000000000000001.2..3...4....5.....5.....5.....5.....5.....5.....5.
```

Figure 4.5: Deterministic outflow from a traffic jam.

```
02...4........5.........5.........5.........5.........5.........5....
1..3......5.........5.........5.........5.........5.........5.........
02...4........5.........5.........5.........5.........5.........5....
1..3......5.........5.........5.........5.........5.........5.........
02...4........5.........5.........5.........5.........5.........5....
1..3......5.........5.........5.........5.........5.........5.........
02...4........5.........5.........5.........5.........5.........5....
1..3......5.........5.........5.........5.........5.........5.........
02...4........5.........5.........5.........5.........5.........5....
```

Figure 4.6: Acceleration from a dense situation (open system). Particles are inserted with maximum speed at the left boundary whenever there is space, but due to the other particles ahead they are immediately slowed down. In consequence, the system is not able to reach its maximum throughput.

4.4 Summary

Already a deterministic CA model for traffic, which is a subcase of the full model, shows some features which are realistic for traffic. Light traffic is characterized by holes moving with the traffic; dense traffic is characterized by kinematic jam waves moving backwards against the traffic. The regimes are separated by a relatively obvious phase transition, showing diverging relaxation times after disturbances.

This transition point gets additional importance because it is automatically selected as output from a jam.

As will be shown in the next chapters, this model already captures some of the features of traffic jam dynamics. It has, though, the property that outflow traffic is maximally dense, in the sense that at any higher density, cars could no longer move at maximum speed. Yet, outflow traffic which is not "maximally" dense is the additional necessary ingredient for traffic jams becoming the singular clusters which they are in traffic measurements (Fig. 3.1).

```
05.....5.....5.....5.....5.....5.....5.....5.....5.....5.....5.....5..
5.....5.....5.....5.....5.....5.....5.....5.....5.....5.....5.....5...
4....5.....5.....5.....5.....5.....5.....5.....5.....5.....5.....5....
3...5.....5.....5.....5.....5.....5.....5.....5.....5.....5.....5.....
         x   (disturbance)
2..5.....4.....5.....5.....5.....5.....5.....5.....5.....5.....5.....5
1.5.....4....5......5.....5.....5.....5.....5.....5.....5.....5.....5.
05.....4....5.....5......5.....5.....5.....5.....5.....5.....5.....5..
5.....4....5.....5.....5......5.....5.....5.....5.....5.....5.....5...
4....4....5.....5.....5.....5......5.....5.....5.....5.....5.....5....
3...4....5.....5.....5.....5.....5......5.....5.....5.....5.....5.....
```

Figure 4.7: Acceleration from a dense situation (open system) with a forced acceleration of the leftmost particle. This means that at this position, a particle instantly can accelerate from zero to, e.g., the maximum speed five (see, e.g., from the first to the second line).

Chapter 5

Cruise control limit and self-organized criticality

Already in Chapter 3 it became clear that start-stop-waves play an important role, as well in the model behavior as in reality. Chapter 4 then established that dense traffic can be distinguished from light traffic by the direction of the wave speed, and that the transition point between the regimes is the point of maximum flow.

This chapter now continues to work out the relation between the waves and the flow maximum. It actually starts with observations of the full model of Chapter 3, but then moves to a "cruise control limit", where the picture is clearer. Nevertheless, this cruise control limit correctly captures the main features of the dynamics of the full model. The exact relation between the cruise control limit and the full model will then be described in Chapters 6 & 7.

5.1 Density waves

Contrary to the deterministic model of the last chapter, the original model reaches its much lower maximum throughput $q_{max} = 0.318 \pm 0.001$ already at a density of $\rho(q_{max}) = 0.086 \pm 0.002$ (Fig. 3.6). What is the deeper reason behind this capacity limitation?

As a first step, one can look at space-time-plots of systems slightly below and above the threshold density $\rho(q_{max})$ (first row of Fig. 5.1). As before, in these pictures horizontal lines are configurations at consecutive time steps, time evolving downwards. Black pixels stand for occupied sites. Vehicles are moving from left to right, and by following the pixels, one can discern the trajectories of the vehicles.

These pictures show marked shock waves, and they occur more often for the higher density. The waves form at arbitrary times and positions due to a "bad" superposition of the disturbances caused by the random element in the velocity update. They are clearly visible as clusters of cars of low velocity, with more interior structure inside the clusters. Once such a disturbance has formed, it is maintained as long as there are more vehicles arriving at the end of the queue than vehicles leaving the queue at its head. These disturbances appear already well *below* the regime of maximum traffic flow, but they are rare. They start to dominate the system's appearance at densities above the regime of maximum flow. This leads to the idea that the regime of maximum traffic flow might be reached when there are, for the first time, waves with a "very long" lifetime, similar to a percolation transition [163]. See also Ref. [167] for a similar analysis of a deterministic model.

Figure 5.1: (Previous page) Plots of simulated single lane freeway traffic in the space-time-domain with resolutions (a) 1:1, (b) 1:4, (c) 1:16. *Left column:* Density $\rho = 0.07$, slightly below the regime of maximum flow. *Right column:* Density $\rho = 0.1$, slightly above the regime of maximum flow. Each black pixel corresponds to a site occupied by a vehicle at a certain place (x-direction) and at a certain time (y-direction). A trajectory of an undisturbed vehicle goes therefore diagonally downwards and to the right. The pictures of the first row cover 500 sites and 500 time steps. The pictures of each row are contained (as indicated by the boxes) in the pictures of the row underneath.

To get a better overview, the second and third row of Fig. 5.1 show the same system at lower resolutions obtained by averaging, therefore showing a larger part of the system and more time steps. A striking feature of these pictures is that they look in some way self-similar [41, 106], i.e., large jams are composed of many smaller ones which look like large ones at a higher resolution. This supports the idea of a critical transition at maximum flow.

5.2 The cruise control limit

To analyse these jam-clusters, it is extremely helpful to construct a system where at most one such cluster exists. This is achieved by taking the “cruise control limit” of the model: Fluctuations at free driving are set to zero. The resulting model reads as follows: For every configuration of the model, one iteration consists of the following steps, which are each performed simultaneously for all vehicles (the quantity gap again equals the number of empty sites in front of a vehicle):

- A vehicle is stationary when it travels at maximum velocity v_{max} and has free headway ($gap \geq v_{max}$). Such a vehicle just maintains its velocity.
- If a vehicle is not stationary, it is jammed. The following two rules are applied to jammed vehicles:
  - **Acceleration of free vehicles:** If a vehicle has $gap \geq v+1$, then: With probability $1/2$, it accelerates to $v+1$, otherwise it keeps the velocity v.
  - **Slowing down due to other cars:** Each vehicle with $gap \leq v$ slows down to gap: $v := gap$. With probability $1/2$, it over-reacts and slows down even further: $v := \max[gap-1, 0]$.
- **Movement:** Each vehicle advances v sites.

For clarity, a formal version of the velocity update is given in the appendix.

While in the original model (Chapter 3), vehicles at v_{max} slow down randomly with probability $p_{free} = p$, here only the jammed vehicles move nondeterministically. This corresponds to the $p_{free} \to 0$ limit, or the “cruise control limit”, of the original model and completely separates the time scales for driving (i.e. perturbing) the system and the system's response.

The fundamental diagram, or current-density relation, $q(\rho)$, was determined numerically as shown in Fig. 5.2 for a closed system of size $L = 30\,000$. Starting with a random initial condition with N cars (i.e. $\rho = N/L$) and after discarding a transient period of $5 \cdot 10^5$ iterations, we measured $\langle q \rangle_L(t) = \sum_{i=1}^{N} v/L$ every 2500 time-steps up to the $3 \cdot 10^6$th iteration. Each data point corresponds to the average over current measurements for a single initial condition, with the following exception: When a run becomes stationary (i.e. no more jammed cars in the sense of the definition above), then the future behavior is predictable. In this case, the run is stopped, and the current will be equal to $q_{det} = v_{max} \cdot \rho$, see below.

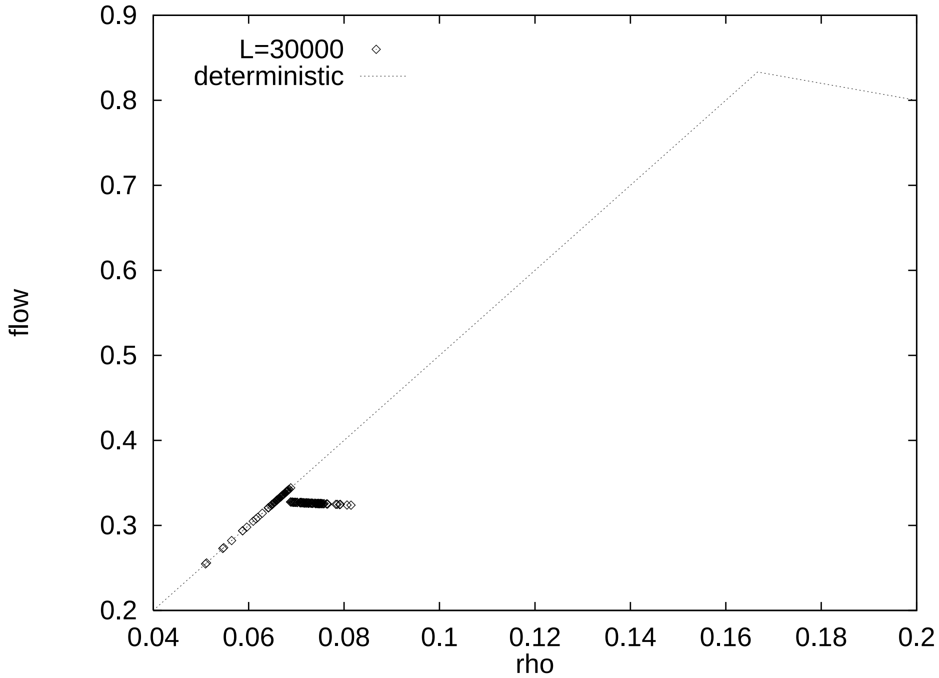

Figure 5.2: The fundamental diagram, $q(\rho)$, for $v_{max} = 5$. The dotted line is valid for deterministic traffic, i.e. when the initial state is prepared such that for each car $gap > v_{max}$ and $v = v_{max}$. The points are measurement results starting from random initial conditions; each point corresponds to one run of a closed system of length $L = 30\,000$ and an average over $2.5 \cdot 10^6$ iterations. When a run relaxed to the deterministic state (no more jammed cars), it was stopped and the deterministic current was taken as the result (points on the dotted line).

For a spatially infinite system, the following results hold: For $\rho < \rho_c$, jams present in the initial configuration are eventually sorted out and the stationary deterministic state is jam free with every vehicle moving at maximum velocity. Thus in the lamellar regime the current is a linear function of density with slope $v_{max} = 5$. Lamellar behavior is observed up to a maximum current $q_c(\rho_c)$. For $\rho > \rho_c$, and $\rho < \rho_{det,max}$ (defined below) the system is bistable. Starting from an initial configuration which has many jams, the jams in this case are never sorted out (infinite system size). The steady state is an inhomogeneous mixture of jam free regions and higher density jammed regions. Clearly, these jammed regions decrease the average current in the system. It is possible, nevertheless, to prepare initial configurations that have no jams. Since all motion is deterministic in this state, the steady state will also have no jams and the current will still be a linear increasing function of ρ (the dotted line in Fig. 5.2). This is possible up to densities of

$$\rho_{det,max} = \frac{1}{v_{max} + 1} ,$$

leading to a maximum current of

$$q_{det,max} = \frac{v_{max}}{v_{max} + 1} .$$

This clearly is much higher than the current q_c for random initial conditions. It is in this sense that our system is bi-stable (cf. also [148, 167]). This effect allows us to produce outflows with densities above ρ_c.

Above ρ_c, the current-density relation can be derived by assuming that the system phase separates into jammed regions separated by jam free gaps. The jam free gaps are the outflow of a jam and thus have current $q_c(\rho_c)$, as argued in the next section. Conservation of the number of cars and of volume leads to $N_f + N_j = N$, $L_f + L_j = L$, $N_j/L_j = 1/a$, $N_f/L_f = \rho_c$, where N_f,L_f, and ρ_c are the number, length, and density, respectively, in the free flowing phase, and N_j, L_j, and $1/a$ are the corresponding quantities in the jammed phase. After some algebra one obtains

$$q = q_c - \frac{(\rho - \rho_c)(aq_c - v_j)}{1 - a\rho_c} \quad ,$$

where a is the average number of lattice sites per jammed vehicle, and v_j is the average velocity ($< v_{max}$) of a jammed vehicle (see [10] for a similar calculation). Thus, the current-density relation is linear both above and below the critical point, as demonstrated in Fig. 5.2.

The discontinuity in the current at the critical point, as seen in the figure, is a finite size effect due to the fact that each point in the figure represents a single initial configuration. In a finite system, there is a finite probability that even a system with supercritical density $\rho > \rho_c$ finds the deterministic state, and then has a current of $q_{det} > q_c$.

5.2.1 The outflow from a jam occurs at maximum throughput

A striking feature of the model is that maximum throughput is selected automatically when the left boundary condition is an infinitely large jam and the right boundary is open. An intuitive explanation is that maximum throughput cannot be any higher than the intrinsic flow rate out of a jam, because then jams become stable in the long time limit and reduce the overall current. By definition, of course, maximum throughput cannot be lower than this intrinsic flow rate.

In Fig. 5.3, the cars on the left flow out from a region of high density where they move with zero velocity. This high density region is not plotted here; only the interface or front separating the high density region and its deterministic outflow is plotted. This is the branched structure on the left hand side of the figure. The vehicles flowing out of the large jam ultimately relax to the deterministic state when they have moved sufficiently far away from the jam.

This feature of maximum throughput selection is a general feature of driven diffusive systems [21, 34, 86]. However, in our case the left boundary condition is unusual: if the left boundary is fixed in space as in [21, 34, 86], then the outflow from a jam cannot reach maximum throughput (cf. bottleneck situation in the last and in the next chapter).

5.2.2 Traffic jams in the outflow show self-organized criticality

The outflow situation, as described above, produces deterministic flow asymptotically at large distances. This means that sufficiently far downstream from the large jam, the jam flow has sorted itself out into deterministic flow. In the deterministic region, one car is randomly perturbed by reducing its velocity to zero. Many different choices for the local perturbation, however, give rise to the same large scale behavior. The perturbed car eventually re-accelerates to maximum velocity. In the meantime, though, a following car may have come too close to the disturbed car and has to slow down. This initiates a chain reaction – the emergent traffic jam.

Fig. 5.3 shows the first 1400 time steps of such an emergent jam (the right jam in the figure). Qualitatively, the jam clearly shows a tendency to branch with complex internal structure and a fractal appearance. The emergent traffic jams drift backwards; so it is possible for a sufficiently long lived emergent jam to eventually intersect with the outflow jam interface that is itself becoming broader

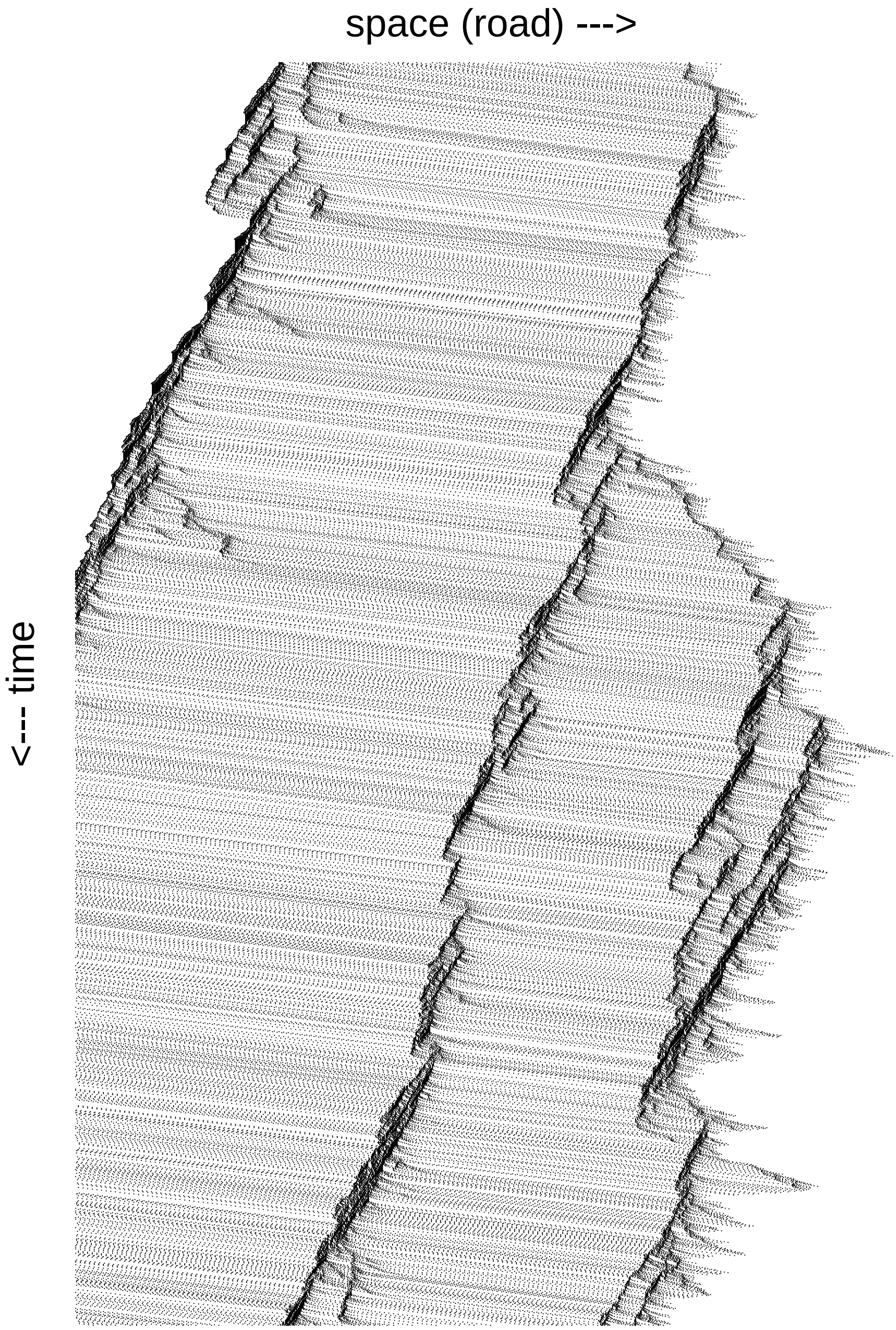

Figure 5.3: Outflow from a dense region (left); this outflow relaxes precisely to the critical density. In the outflow region, a jam is triggered by a small disturbance. Note the branching behavior of this jam. — "Deterministic" vehicles to the right of the jam are not plotted.

with time. It is likely that the branching behavior of the emergent jams is the same as the branching behavior of the original jam interface. In this work, however, we do not explicitly study the interface. Contrary to the figure, in the computer code, the interface region to the left and the jam to the right are kept completely separate using methods described in the appendix.

A jam is sorted out when the number of jammed cars is zero. This defines the lifetime, t, of an emergent traffic jam. In order to obtain statistics for the distribution of traffic jam lifetimes, $P(t)$, for example, the deterministic outflow is then disturbed again. Other cluster statistics such as the spatial extent w of the jam or overall space-time size s (mass) of the jam are obtained as well. These distributions are analogous to similar distributions for other branching processes such as directed percolation [49], branching annihilating random walks [76], or in nonequilibrium lattice models [75] although the precise behaviors are different.

Fig. 5.4 shows 1400 time steps in the middle of the life of a larger jam. Here, vehicles that are stationary are no longer shown; the plot only shows the "particles", or jammed vehicles, that propagate the disturbance.

For a quantitative treatment, we start by measuring the probability distribution of jams as a function of their lifetime t. Fig. 5.5 shows that for $t >\sim 100$ this distribution follows a power law

$$P(t) \sim t^{-(\delta+1)} \qquad \text{with} \qquad (\delta+1) = 1.5 \pm 0.01 \ ,$$

very close to $\delta = 1/2$. Figure 5.5 represents averaged results of more than 60 000 avalanches.

Here scaling is observed over almost four orders of magnitude as determined by our *numerically imposed* cutoff: For this figure, if jams survive longer than 10^6 time steps, they are removed from the data base. It is very important to note that these emergent jams are precisely critical. Their power law scaling persists up to any arbitrarily large numerically imposed cutoff. The lifetime distribution is related to the survival probability $P_{surv}(t)$ by

$$P_{surv}(t) = \int_t^\infty \mathrm{d}t' P(t') \sim t^{-\delta} \qquad \text{for} \qquad \delta > 0 \ .$$

We again emphasize that no external tuning is necessary to observe this scaling behavior. The outflow from the infinite jam self-organizes to the critical state.

5.3 Random walk arguments

Paczuski [123] has developed a phenomenological theory for the branching waves. The arguments are given in this and the next section.

It is, perhaps, surprising that such a seemingly complicated structure as shown in Fig. 5.3 is described by such a simple apparent exponent. Numerically, the exponent $\delta + 1$ is conspicuously close to $3/2$, the first return time exponent for a one-dimensional random walk. In fact, for $v_{max} = 1$ this random walk picture is exact, as shown below.

Let us consider a single jam in a large system with $v_{max} = 1$. The vehicles in the jam form a queue, and all of these cars have velocity zero. When the vehicle at the front of the jam accelerates to velocity one, it leaves the jam forever. The rate at which vehicles leave the jam is determined by the probabilistic rule for acceleration. Vehicles, of course, can be added to the jam at the back end. These vehicles come in at a rate which depends on the density and velocity of cars behind the jam. Given the rules for deceleration, the spacing between the jammed cars is zero so that the number of cars in

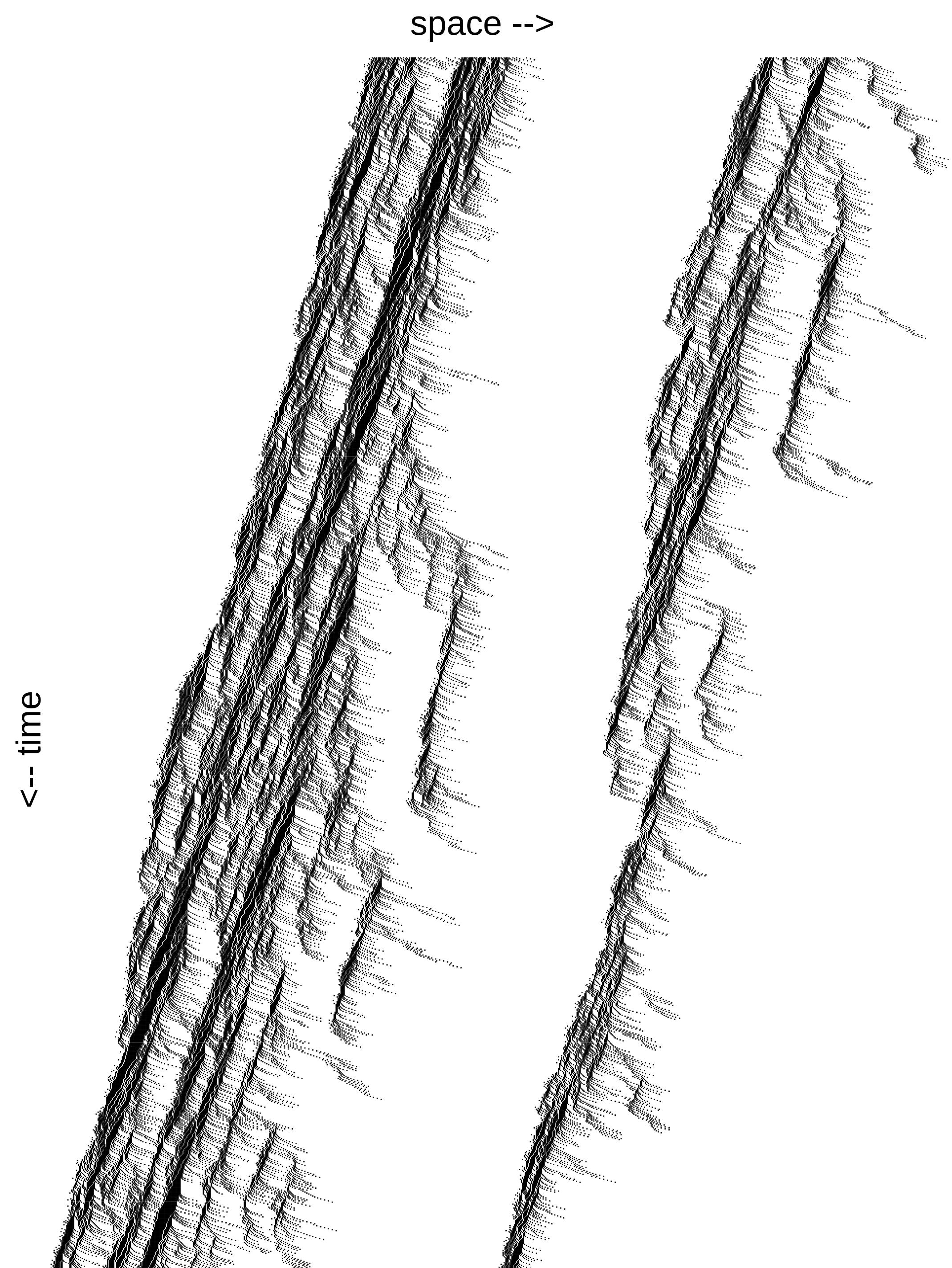

Figure 5.4: Space-time plot of a huge emergent jam. Only vehicles with $v < v_{max}$, i.e. "jammed cars", are plotted.

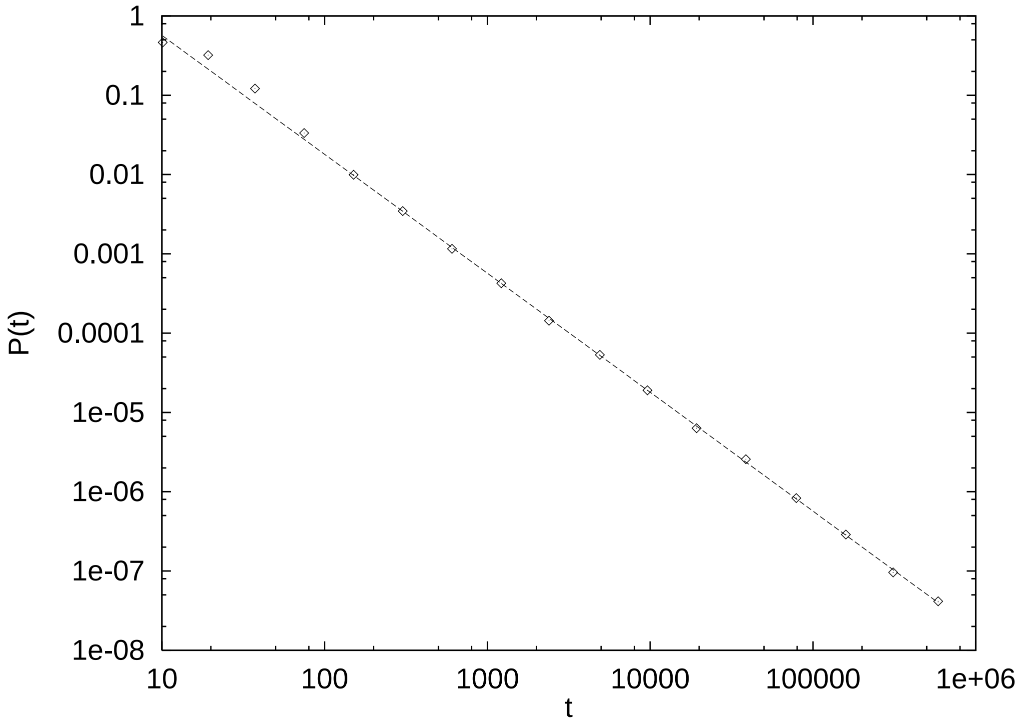

Figure 5.5: Lifetime distribution $P(t)$ for emergent jams in the outflow region; average over more than 65 000 clusters (avalanches). The straight line has slope 3/2. Without external tuning, the lifetime distribution is precisely critical up to the numerically imposed cut-off at $t = 10^6$.

the jam, n, is equal to the spatial extent of the jam, w. This contrasts with the branching behavior for $v_{max} > 1$. The probability distribution, $P(n,t)$, for the number of cars in the jam n at time t is determined by the following equation:

$$P(n, t+1) = (1 - r_{in} - r_{out})P(n,t) + r_{in}P(n-1,t) + r_{out}P(n+1,t) \quad . \qquad (*) \tag{5.1}$$

Here, the quantities r_{in} and r_{out} are phenomenological parameters that depend on the density behind the jam and the rate at which cars leave a jam. They are independent of the number of cars in the jam. For large n and t, one can take the continuum limit of Eqn. $(*)$ and expand to lowest order

$$\frac{\partial P}{\partial t} = (r_{out} - r_{in})\frac{\partial P}{\partial n} + \frac{r_{out} + r_{in}}{2}\frac{\partial^2 P}{\partial n^2} \quad . \tag{5.2}$$

When the density behind the jam is such that the rate of cars entering the jam is equal to the intrinsic rate that cars leave the jam, then the first term on the right hand side vanishes. Then, the jam queue is formally equivalent to an unbiased random walk in one dimension [42]. The first return time of the walk then corresponds to the lifetime of a jam. This leads immediately to the result $P(t) \sim t^{-3/2}$ for the lifetime distribution.

This argument shows that the outflow from an infinite jam is in fact self-organized critical. This can be seen immediately by noting that the outflow from a large jam occurs at the same rate as the outflow from an emergent jam created by a perturbation. This also shows that maximum throughput corresponds to the percolative transition for the traffic jams. Starting from random initial conditions in a closed system, the current at long times is determined by the outflow of the longest-lived jam in the system.

When $r_{in} = r_{out}$, one also finds from Eqn. (*) that $n \sim t^{1/2}$ and the size of the jam $s \sim nt \sim t^{3/2}$. If the density in the deterministic state is below the critical density ρ_c, then the jams will have a characteristic lifetime, t_{co}, size s_{co}, number n_{co}, etc. From Eqn. (*), $t_{co} \sim n_{co}(r_{out} - r_{in})^{-1}$. Assuming that near the critical point $r_{out} - r_{in} \sim \rho_c - \rho$, then using $n_{co} \sim t_{co}^{1/2}$ leads to

$$t_{co} \sim (\rho_c - \rho)^{-2} \quad .$$

For $\rho > \rho_c$, vehicles on average enter the jam at a faster rate than they leave. In this case, there is a finite probability to have an infinite jam, P_∞, which vanishes as $\rho \to \rho_c$ as

$$P_\infty \sim (\rho - \rho_c)^{\tilde{\beta}} \quad .$$

The steady-state density of jammed cars, $\rho_j = (\rho - \rho_c)^1$, so that the order parameter exponent $\tilde{\beta} = 1$.

From the random walk Eqn. (*), and in analogy with other branching processes such as directed percolation [49], P_{surv} follows a scaling form

$$P_{surv}(t, \Delta) \sim t^{-\delta} f(t\,\Delta^{\nu_t}) \ ,$$

near the critical point. Here $\Delta \equiv |\rho - \rho_c|$ and $t_{co} \sim \Delta^{-\nu_t}$. From this scaling relation, $\tilde{\beta} = \delta\nu_t$. For $v_{max} = 1$, $\delta = 1/2$, $\nu_t = 2$, and $\tilde{\beta} = \beta = 1$.

The number of jammed vehicles, $\bar{n}$, averaged over all jams, including those that die out, has the scaling form

$$\bar{n} \sim t^{\eta} g(t\,\Delta^{\nu_t}) \ .$$

The number of jammed vehicles averaged over surviving jams, scales with a different exponent

$$n(t) = \bar{n}(t)/P(t) \sim t^{\eta+\delta} \ .$$

The mapping to the random walk gives $\eta = 0$.

The cluster width, averaged over surviving clusters, scales as $\bar{w} \sim t^{1/z}$, and the mapping to the random walk gives $z = 2$. The average cluster size $\bar{s} \sim t^{\eta+\delta+1}$; $\bar{s} \sim t^{3/2}$ in the random walk case.

In the numerical measurements, we averaged the quantities t = lifetime of the cluster, w = maximum width of cluster during cluster life, n = maximum number of simultaneously jammed vehicles during cluster life, s = total number of jammed vehicles during cluster life.

Our theoretical results should describe the emergent traffic jams not only at $v_{max} = 1$ but also for any $v_{max} > 1$ as long as the traffic jam itself remains dense. If this is the case, then the dynamical evolution is determined solely by the balance of incoming and outgoing vehicles as described by Eqn. (*). The ratio $\bar{w}/n$ should go to a finite constant at large times if the theory is valid. If the emergent jams break up into a fractal structure, and $\bar{w}/n$ diverges, internal dynamics must also be included. Since the jams displayed in Figs. 5.3 and 5.4 appears branched and at least qualitatively fractal, one might doubt that such a simple theory could describe this behavior. Nevertheless, the close numerical agreement of the lifetime distribution exponent for the SOC behavior suggests the possibility that the random walk theory is a valid description of the branching jam waves.

5.4 A cascade equation for the branching jams

We now analyze the branching behavior of jams with $v_{max} > 1$ in terms of a phenomological cascade equation. A very large emergent jam, at a fixed point in time, consists of small dense regions of jammed cars, which we call subjams, separated by intervals, "holes", where all cars move at maximum velocity. If the jam is dense, then the holes have a finite average size. Otherwise, the jammed vehicles comprise a fractal with dimension $d_f < 1$. We will consider the subjams to have size one.

Holes between the subjams are created at small scales by the probabilistic rules for acceleration. Each subjam can create small holes in front of it. We will ignore the details of the injection mechanism, and assume that there is a steady rate at which small holes are created in the interior of a very long lived jam. We also assume that the interior region of a long-lived jam reaches a steady state distribution of hole sizes.

In order to determine the asymptotic scaling of the large holes in the interior of a long-lived jam, it is necessary to isolate the dominant mechanism in the cascade process for hole generation. The microscopic mechanism that connects holes at different scales is the dissolution of one subjam. When one subjam dissolves because the cars in it accelerate to maximum velocity, the two holes on either side of it merge to form one larger hole. Holes at any large scale are created and destroyed by this same process. In the steady state, the creation and destruction of large holes must balance. This leads to a cascade equation for holes of size x:

$$\sum_{u=x+1} < h(x)h(u-x) >= \sum_{x'=1}^{x-2} < h(x')h(x-x'-1) > \quad . \qquad (**)$$

Here, the angular brackets denote an ensemble average over all holes in the jam, and the quantity $h(x)h(u-x)$ denotes a configuration where a hole of size x follows a hole of size $u-x$. The right hand side of this equation represents the rate at which holes of size x are created, and the left hand side represents the rate at which holes of size x are destroyed.

Now, we make an additional ansatz; namely, for large x, $< h(x')h(x-x'-1) >= G(x)$, independent of x' to leading order. That is, to leading order the probability to have two adjacent holes, whose sizes sum to x is independent of the size of either hole. $G(x)$ then also scales the same as $P_h(x)$, the probability to have a hole of size x. Thus Eqn. $(**)$, to leading order can be written

$$xG(x) \sim \sum_{u=x} G(u) \quad .$$

Differentiating leads to

$$x\frac{\partial G(x)}{\partial x} = -2G(x) \quad ; \quad G(x) \sim \frac{1}{x^2} \quad .$$

Thus the distribution of hole sizes decays as

$$P_h(x) \sim x^{-\tau_h} \quad ; \quad \text{with} \tau_h = 2 \quad .$$

It is interesting to note that the cascade equation $(**)$ is identical to the dominant mechanism in the exact cascade equation for forests in the one-dimensional forest fire model [128]. In addition, the result $\tau_h = 2$ equals the distribution exponent for the forests, which has been obtained exactly [35, 128].

The exponent τ_h is related to the fractal dimension d_f of jammed vehicles by

$$\tau_h = 1 + d_f \ ,$$

as long as $\tau_h \leq 2$ [107]. Thus, $\tau_h < 2$ implies that the equal time cut of the jam clusters is fractal, otherwise not. The point $\tau_h = 2$ is the boundary between fractal and dense behavior. At this special point, the random walk theory can still be expected to apply, although with logarithmic corrections.

The width of an emergent jam, at a given point in time, $w(t)$, can be expressed as

$$w(t) = \frac{n(t)}{w_j}\left(w_j + \int \mathrm{d}x\, x\, P_h(x,t)\right) \quad .$$

Here, w_j is the average width of a subjam, it is $\mathcal{O}(1)$. The quantity $P_h(x,t)$ is the probability distribution to have a hole of size x in a jam that has survived to time t. It is natural to assume that this distribution corresponds to $P_h(x)$ up to a cutoff which grows with t. Inserting the expression for $P_h(x)$ gives

$$w(t) \sim n(t)\left(1 + \int_1^{x_h^*} \mathrm{d}x\, x^{1-\tau_h}\right) \quad ,$$

where the upper bound x_h^* represents a time-dependent cutoff. Using $\tau_h = 2$, $n \sim t^{\delta+\eta}$, and assuming $x_h^* \sim t^c$ gives

$$w(t) \sim t^{\delta+\eta}\,(1 + c\,\log t) \qquad \text{for } \tau_h = 2 \quad .$$

In other words, if $\tau_h = 2$, as the above arguments suggest, spatial quantities such as $w(t)$ will exhibit logarithmic corrections to the random walk results. In the following section, we test these theoretical predictions with further numerical studies.

5.5 Simulation results

In this section, we present the rest of our numerical results. Unless otherwise noted, these results were obtained for systems with $v_{max} = 5$.

5.5.1 At the self-organized critical point

We study the critical properties of the outflow of a large jam by driving it with slow random perturbations as described in Sec. II. Numerically, we find (Fig. 5.6)

$$n(t) \equiv \langle\, n\,\rangle_{surv}(t) \sim t^{\eta+\delta} \qquad \eta + \delta = 0.5 \pm 0.1$$

and (Fig. 5.7)

$$s(t) \sim n(t)t \sim t^{1+\eta+\delta} \qquad 1 + \eta + \delta = 1.5 \pm 0.1$$

in agreement with the random walk predictions. However, the simulations do not converge to power law scaling before $t \simeq 3 \cdot 10^4$, and since the simulation is cut off at $t = 10^6$, the exponents are obtained from less than two orders of magnitude in t. Figs. 5.6 and 5.7 contain the averaged results of more than 160 000 avalanches, typically corresponding to approximately 200 workstation hours (see Appendix and figure captions for further information).

5.5.2 Off criticality

By changing the left boundary condition (i.e. the inflow condition) of the open system, simulations were performed both above and below the critical point. This is achieved by replacing the mega jam by the following mechanism: Vehicles are inserted at a fixed left boundary so that in all cases v_{max}

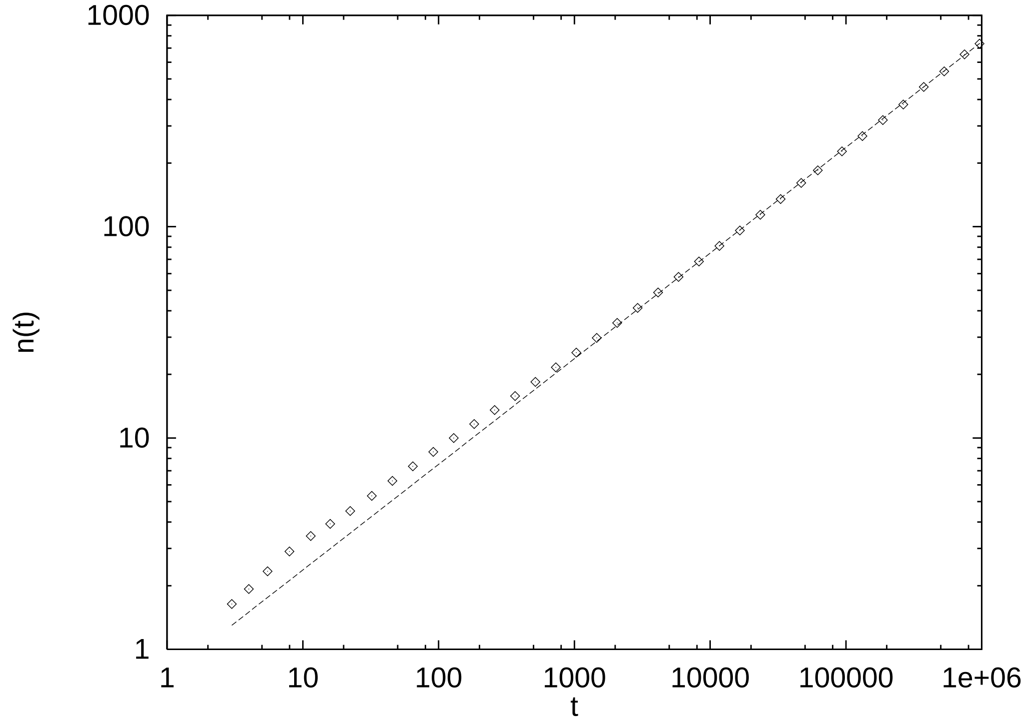

Figure 5.6: Number of jammed particles at time t, $n(t)$, averaged over surviving clusters, in the outflow situation. More than 165 000 clusters were simulated. The straight line has slope 1/2. Note that the measurement only converges for $t >\sim 5000$.

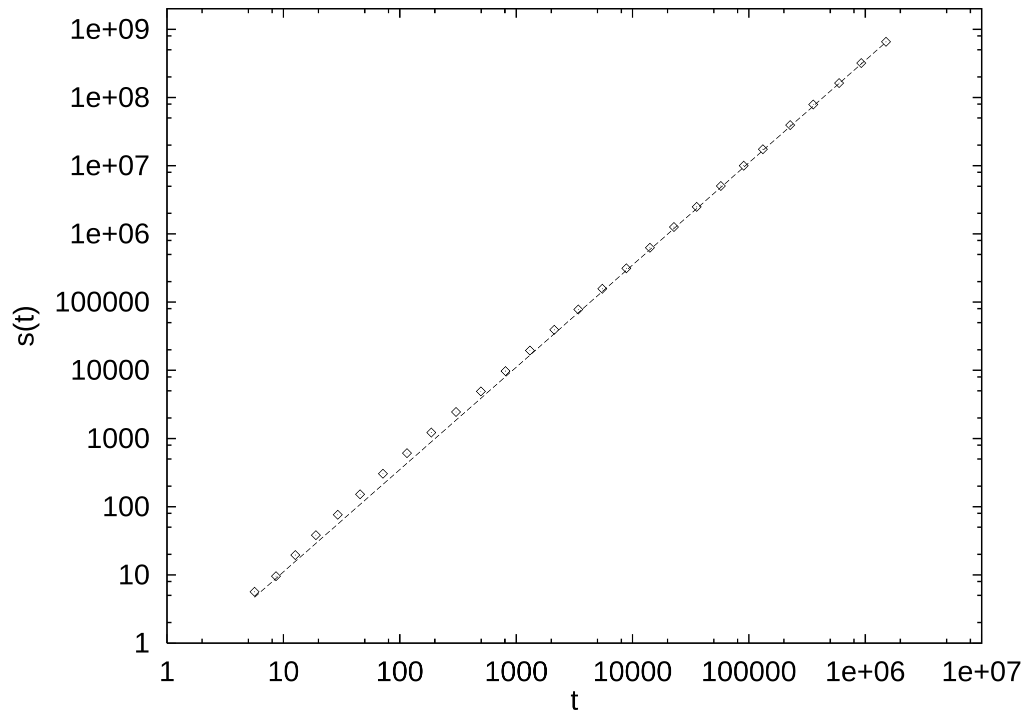

Figure 5.7: Mass of jam in space-time, $s(T)$, in the outflow situation, for the same clusters os in Fig. 5.6. Jams of similar lifetime T were averaged. The straight line has slope 3/2. Note that the measurement again only converges for $t >\sim 5000$.

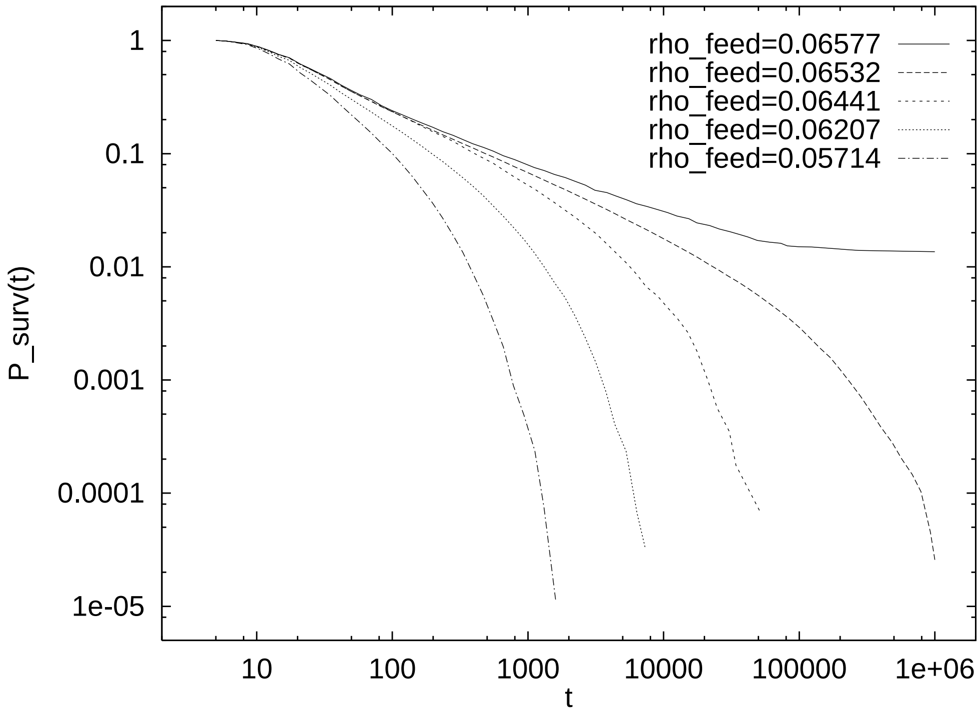

Figure 5.8: Survival probability for jam-clusters, $P_{surv}(t)$, for different inflows. This picture corresponds exactly to the theoretical picture, cf. Fig. 2.1. Note that this distribution is highly sensitive to the inflow, re-confirming that the outflow is indeed precisely critical.

sites are left empty and then the following sites are attempted to be occupied with probability p_{insert} until a site is occupied. The rate p_{insert} determines an average density ρ by

$$\rho = \frac{1}{v_{max} + 1/p_{insert}} ,$$

which can go as high as $\rho = \rho_{det,max} = 1/6 = 0.16666\ldots$ for $v_{max} = 5$, much higher than the critical density of $\rho_c \approx 0.0702$.

We have performed data collapse for the survival probability $P_{surv}(t)$ on varying the density, as shown in Fig. 5.9. By plotting $P_{surv}/t^{-\delta}$ vs. $t\,\Delta^{\nu_t}$ with the exponents $\delta = 0.5$, $\nu_t = 2$ was determined by the qualitatively best collapse. The accuracy of this method is not very high, though, so that the conclusion from the numerical results is no better than

$$\nu_t = 2 \pm 0.2 ,$$

which is again in agreement with our random walk predictions.

5.5.3 Spatial behavior

So far, we have only shown simulation results for exponents describing the evolution of the number of vehicles, but not their distribution in space. Here, our simulation results are less conclusive. The width $\bar{w}(t)$ vs. t (Fig. 5.10) is, besides the convergence problems already described, best approximated by an exponent

$$\frac{1}{z} = 0.58 \pm 0.04$$

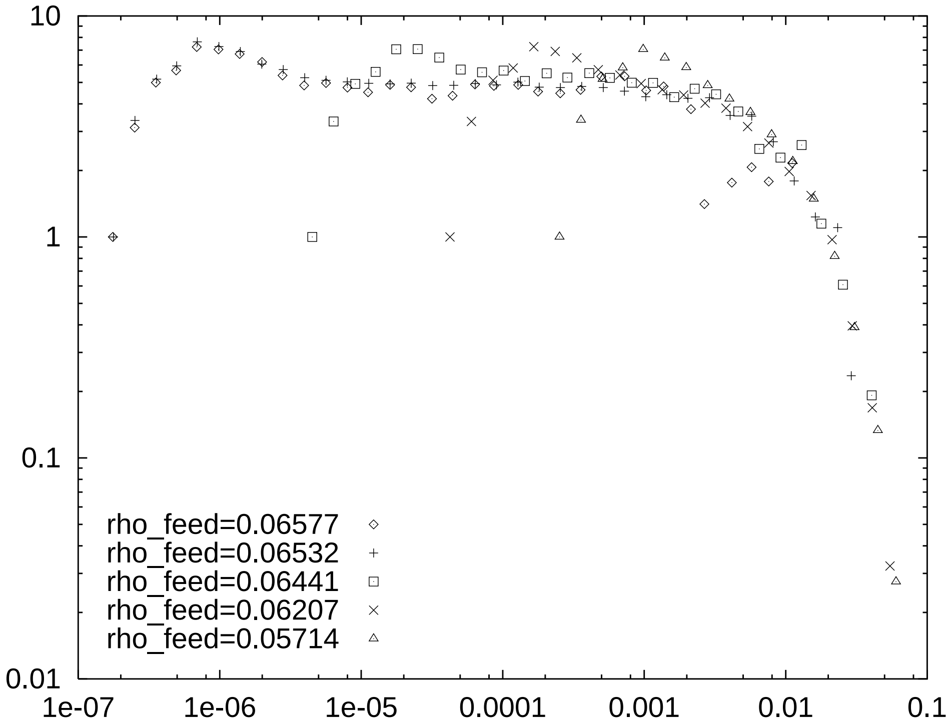

Figure 5.9: Data collaps for the survival probability of jams for the same data as for Fig. 5.8 with $\delta = 0.5$ and $\nu_t = 2$.

instead of 1/2. Measurements of other relations (e.g. w vs. n; not shown) confirm these discrepancies for the spatial behavior for branching jam clusters with $v_{max} > 1$. However, the form $w(t) \sim t^{1/2} \ln t$ vs. t (Fig. 5.10) is also consistent with the numerics.

In an effort to resolve this question, we analyzed large jam configurations. We ran simulations with $v_{max} = 2$ until a cluster reached a width of, say, $2^{13} = 8192$, and stored the configuration of this time-step. About 30 configurations of the same size were used. Box-counting analysis of these configurations was not conclusive, but measuring the distribution of holes inside the configurations is consistent with the results from the cascade equation, presented earlier.

Fig. 5.11 shows a plot of the probability distribution for hole sizes, $P_h(x)$ vs. x, obtained from these configurations. We find

$$P_h(x_h) \sim x_h^{-\tau_h} \qquad \tau_h = 1.96 \pm 0.1 \ ,$$

which is indeed consistent with the prediction $\tau_h = 2$ from the cascade equation.

Nevertheless, our numerical results are not precise enough to distinguish $\tau_h = 2$ from $\tau_h < 2$ for the holes exponent, or the power law fit with exponent 0.58 from the theoretically plausible fit with exponent 1/2 and logarithmic corrections for the width exponent.

5.6 Applications to real traffic

With respect to real world traffic, much of this discussion appears rather abstract. A configuration of size $2^{13} = 8192$, as analyzed in this work, corresponds to more than 100 km of undisturbed roadway, a situation that rarely occurs in reality. However, the following results should be general enough to be important for traffic:

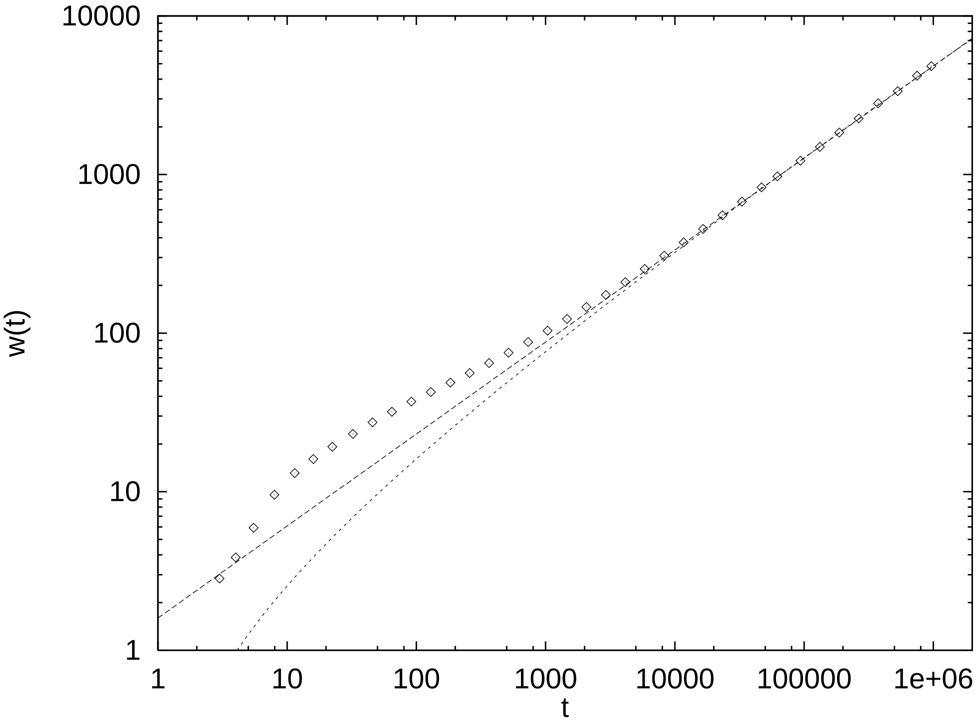

Figure 5.10: Averaged maximum width of clusters, w, as a function of their life-time, t. The straight line has slope 0.58; the dotted line is a logarithmic fit $A \cdot t^{1/2} \cdot \log(t)$ where A is a free parameter. This measurement only converges for life-times $t >\sim 50\,000$, and then, the data material (from the same clusters as for Figs. 5.6 and 5.7 is not enough to distinguish between the scaling law and the theoretically plausible fit with a logarithmic correction.

- The concept of critical phase transitions is helpful for characterizing real traffic behavior. Open systems will tend to go close to a critical state that is determined by the outflow from large jams. This underlying self-organized critical state corresponds to a percolative transition for the jams; i.e. spontaneous small fluctuations can lead to large emergent traffic jams.

- Interestingly, planned or already installed technological advancements such as cruise-control or radar-based driving support will tend to reduce the fluctuations at maximum speed similar to our limit, thus increasing the regime of validity of our results. One unintended consequence of these flow control technologies is that, if they work, they will in fact push the traffic system closer to its underlying critical point; thereby making prediction, planning, and control more difficult.

- The fact that traffic jams are close to the border of fractal behavior means that, from a single "snapshot" of a traffic system, one will not be able to judge which traffic jams come for the same 'reason'. Concepts like point queues [157] or single waves do not make sense when traffic is close to criticality. 'Phantom' traffic jams emerge spontaneously from the dynamics of branching jam waves.

- The fact that holes scale with an exponent around -2 means that, at criticality, the jammed cars are close to not carrying any measure at all. The regime near maximum throughput thus corresponds to large "holes" operating practically at ρ_c and q_{max}, plus a network of branched jam-clusters, which do not change ρ and q very much. The fluctuations found in the 5-minute-measurements of traffic at capacity [2, 56, 69, 132] therefore reflect the fact that traffic flow

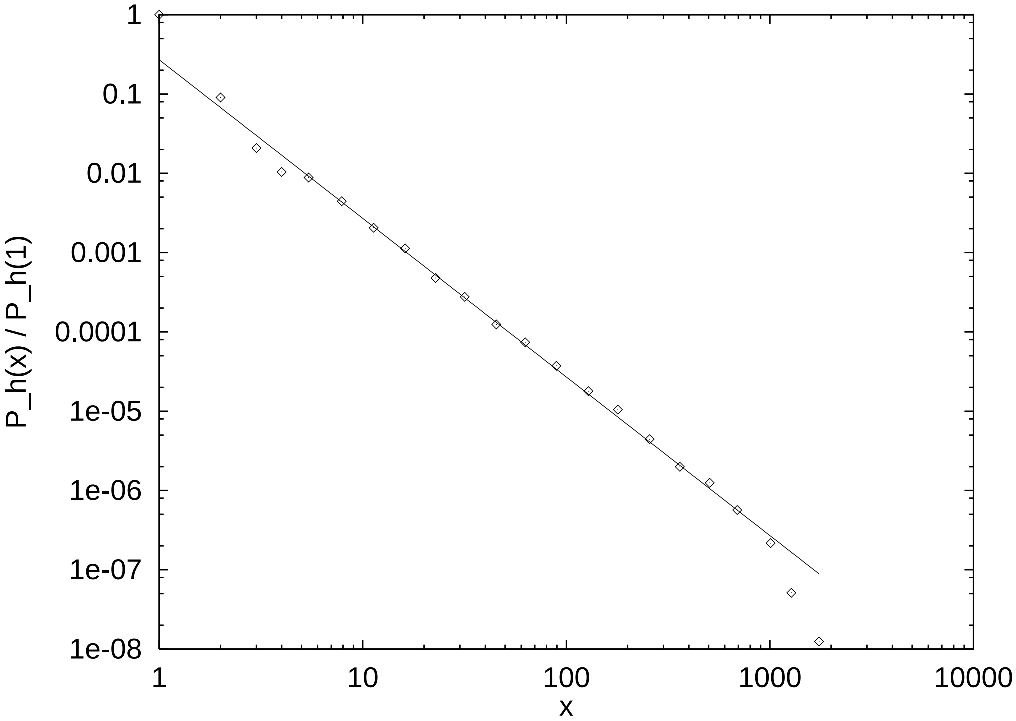

Figure 5.11: Probability distribution P_h for hole-sizes x_h. The straight line has slope -2. The average is over 60 configurations, which all have width $w = 2^13 = 8192$. Contrary to all other figures in this chapter, these results were obtained with $v_{max} = 2$, thus confirming that $v_{max} = 2$ is already sufficient to obtain the described branching behavior.

is inhomogeneous with essentially two states (jammed and maximum throughput). The result of each 5-minute-measurement depends on how many jam-branches are measured during this period.